DYNAMIC INTELLIGENT CHANNEL ASSIGNMENT MODEL WITH OPTIMIZED THROUGHPUT-BASED COGNITIVE UAV GUIDED SMART INTERNET OF THINGS ENVIRONMENT

Reference NO. IJME 2512, DOI: 10.5750/sijme.v167iA2(S).2512

T. Vijaya Kumar*, Research Scholar, Vels Institute of Science, Technology & Advanced Studies, Chennai, TN, India. **Dr. Madona B. Sahaai,** Assistant Professor, Vels Institute of Science, Technology & Advanced Studies, Chennai, TN, India. **Dr. C. Sharanya,** Assistant Professor, Sathyabama Institute of Science and Technology, Chennai, TN, India.

*Corresponding Author: T. Vijaya Kumar (Email): vijaykumar4792@gmail.com

KEY DATES: Submission date: 15.09.2024; Final acceptance date: 23.03.2025; Published date: 30.04.2025

SUMMARY

The IoT technology allows numerous devices to link up with the Internet and exchange data smoothly. It is predicted that shortly, there will be trillions of these devices connected. As a result, there is a growing demand for spectrum to deploy these devices. Many of these devices operate on unlicensed frequency bands, leading to interference as these bands become overcrowded. A new communication approach known as cognitive radio-based Internet of Things (CR IoT) is rapidly emerging to address this issue and the spectrum scarcity. This involves integrating cognitive radio technology into IoT devices, allowing for dynamic spectrum access, and overcoming interference problems. In current systems, a significant portion of the spectrum designated for primary users (PU) may be underutilized, leaving room for secondary users (SU) to utilize the spectrum. However, the main challenge is that SUs must continuously send packets until they find an available channel in real-world conditions, resulting in excessive communication and packet loss. To overcome these kinds of drawbacks in the network in this article dynamic intelligent channel allocation with optimized throughput-based cognitive UAV guided network model is developed. The major categories that are concentrated in this model are UAV-based cognitive IoT network construction, dynamic intelligent channel assignment model, and optimized throughput calculation process. By utilizing these methods, we can achieve streamlined channel allocation and economical communication, ultimately enhancing the performance of the UAV-guided CRN-based IoT environment. The implementation of this model is carried out in MATLAB software and the parameters that are considered for performance analysis are network throughput, power utilization, energy efficiency, data delivery ratio, and average delay.

KEY WORDS: Internet of things (IoT), Cognitive UAV, Unmanned aerial vehicles (UAV), Dynamic intelligent channel assignment

1. INTRODUCTION

The pressing need to address problems related to spectrum scarcity and energy shortages has emerged as a result of the swift growth in wireless traffic during the 5G era. One potential solution is the implementation of cognitive radio networks (CRNs), which can effectively utilize spectrum resources to address the problem of spectrum deficit [1–2]. It is essential for secondary users (SUs) in CRNs to strictly adhere to authorized spectrum usage and ensure that they do not disrupt primary users (PUs) with any unacceptable interference. There exist four primary methods for secondary users to access authorized spectrum: opportunistic spectrum sensing in overlay mode, spectrum sharing in underlay mode, cooperation, and a combination of overlay and underlay modes [3]. In overlay mode, secondary users will only transmit when primary users are not utilizing the spectrum, whereas in underlay mode, secondary users are able to coexist with primary users if their interference remains within acceptable limits [4–5]. In cooperation, SUs act as relays with PUs. The hybrid mode allows for continuous use of the authorized spectrum by adjusting power levels based on PU activity. The hybrid approach is seen as the most versatile and dynamic in terms of optimizing overall spectrum efficiency (SE) when compared to other methods. Moreover, progress in energy harvesting (EH) technology has enabled wireless users to efficiently collect renewable energy sources like solar, wind, and ambient radio frequency (RF) signals [6-8]. This innovation enables users to overcome energy scarcity challenges without relying on conventional fixed batteries or power sources.

The adoption of UAVs in wireless communication has been on the rise as technology has advanced in recent years [9–10]. These UAVs have demonstrated significant promise for a range of purposes, including serving as wireless mobile terminals, base stations, access points,

and relay terminals. Their incorporation into wireless networks can greatly improve connectivity, coverage, and capacity. However, some challenges and tradeoffs need to be considered when using UAVs in cooperative relay systems. One of the main challenges is optimizing the trajectory of the UAVs, which is crucial for ensuring efficient, stable, and safe flight operations [11]. This is especially important when these vehicles are being used as relay terminals in wireless networks. In pursuit of enhancing energy efficiency and extending the longevity of upcoming wireless communication systems, energy harvesting (EH) emerges as a promising strategy that has received considerable attention in the realms of cellular networks and relay selection for cooperative networks [12–13]. Effectively placing drones near individuals is a key obstacle in creating systems that utilize unmanned aerial vehicles (UAVs), as mentioned. Several optimization techniques, such as evolutionary algorithms, have been proposed. Wireless devices have the capability to harness energy from renewable sources or from the RF signals they receive. This phenomenon is referred to as RF-EH, in which energy-constrained wireless devices are capable of harvesting and storing energy from RF signals transmitted by other wireless devices [14]. The phrase IoT, or Internet of Things, denotes a collection of interconnected devices that are linked to the internet, often referred to as IoT devices. These devices possess special identification features and can collect, analyze, and share data online. They can also adjust their usage, deployment, and programming accordingly. In a general sense, IoT devices encompass unconventional computing gadgets located in various settings such as smart homes, offices, environmental monitoring systems, hospitals, industrial automation systems, connected vehicles, remote asset control systems, and more. Such devices have the capability to connect to the Internet and communicate wirelessly.

Wireless communication has been evolving through the utilization of Cognitive Radio (CR), a promising communication model aimed at enhancing the efficiency of the existing radio spectrum. In order to improve spectrum efficiency and tackle possible scarcity concerns in future wireless networks, Cognitive Radio is foreseen to empower radio devices with intelligence for optimal spectrum utilization. Joseph Mitola first introduced CR, followed by an in-depth examination of CR-based Networks (CRNs). By detecting and making use of unused frequency bands, CR enables Secondary Users (SUs) to operate more efficiently. Additionally, CR can sense and monitor surrounding radio environments to determine whether Primary Users (PUs) are present or not. This enables the discovery and use of vacant spectrum gaps or unused communication time slots without causing any disruption to Primary Users (PUs). In IoT-based networks, where many wireless devices require spectrum for their operations, utilizing the limited resources is crucial. As a result of the rapid progress in the wireless communication sector and the extensive use of diverse wireless networks, the radio spectrum is becoming more crowded. However, CR demonstrates significant potential in effectively accommodating many IoT devices in the current spectrum. The article explores the research challenges, open issues, and future directions for CIoT networks in depth. Effectively utilizing the available radio resources poses a major challenge in upcoming cooperative CIoT networks.

2. RELATED WORKS

In [15], the use of multi-antenna UAV-mounted relays and NOMA enhances IoT device performance. Results indicate better outcomes with more antennas, SNR, and fading severity compared to OMA schemes. In [16], the combination of UAVs and wake-up radios in remote IoT applications outperforms six benchmark routing protocols, enhancing network stability, energy efficiency, and data collection. In [17], an optimized UAV formation tracking using deep reinforcement learning and the proposed DIDDPG algorithm for communication delay mitigation. In [18], using UAVs to deploy small cells in hard-to-reach areas for wireless coverage, focusing on optimizing energy use through efficient scheduling. In [19], enhancing performance in simulations is achieved by employing a strategy involving deep reinforcement learning for offloading UAV tasks in power inspection to mobile edge computing servers. In [20], an energy-efficient optimization method for deploying UAVs in IoT data collection uses new encoding for stop points and combines DEoPS and GBoPS techniques. Results show each excels in different areas. In [21], a novel cross-layer computing framework combined with a deep learning-based offloading algorithm enhances performance in power IoT by as much as 20. 73%. In [22], improving IoUT communication with deep reinforcement learning, integrating renewable energy, reducing hops, and addressing interference challenges. In [23], developing a cooperative UAV-assisted task offloading system can optimize energy efficiency and task distribution in disaster areas. Simulation results show significant energy savings and improved performance. In [24], a UAMS for 6G networks balances costs and service needs, enhances migration efficiency, and improves system performance.

In [25], the utilization of blockchain technology in UAV-assisted IoT data collection systems bolster security and improves energy efficiency. Unmanned Aerial Vehicles function as edge nodes, utilizing charging tokens for recharging purposes and employing an adaptive linear prediction algorithm to decrease energy usage. The simulation results confirm the effectiveness of the system. In [26], the algorithm enhances resource management and pricing within a BaaS-MEC system through facilitating information exchange among base stations. It employs a combination of hierarchical reinforcement learning techniques, including deep Q-learning and Bayesian deep learning, to achieve convergence. In [27],

methods are proposed to enhance data rates in molecular communication by utilizing multiple emitters and detectors with algorithms. In [28], a routing protocol designed for UAVs in IoT applications that focuses on energy efficiency seamlessly combines extensive data aggregation with rapid point-to-point communication. In [29], a UAV-enabled MEC network structure uses a cooperative computation offloading scheme with interference mitigation. In the IoT environment, deep reinforcement learning improves utility by optimizing offloading decisions and resource management. In [30], a novel UAV-centered IoT network has been suggested for effective data gathering and three-dimensional device locating. A DE-based optimization method minimizes energy consumption and improves performance compared to traditional networks. In [31], utilizing UAVs and delay-tolerant networking protocols enables data collection from IoT devices across extensive regions even without established infrastructure. A path planning algorithm is proposed for efficient UAV flight paths. In [32], energy efficiency optimization for UAV–based communication networks are the focus of this study, despite uncertainties. A convex optimization scheme with closed-form resource allocation expressions is proposed, which performs well in simulations. In [33], a NOMA-based cognitive UAV communication system to tackle spectrum scarcity with a joint optimization algorithm. In [34], a reconfigurable intelligent surface, known as RIS, enhances a UAV-assisted cognitive radio system by mitigating blocked line-of-sight channels. Enhancing achievable rates for secondary receivers is improved by optimizing UAV trajectory, transmit power, and RIS phase shifts. The simulation has verified its effectiveness.

In [35], the goal of secure RSMA cooperation schemes for maritime cognitive UAV networks is to optimize transmission rate, considering primary privacy and quality of service. A CPFS algorithm improves the transmission rate compared to traditional schemes. In [36], energy-harvesting UAVs combine with CR tech for dependable communication. Analytics on residual energy, connection outages, and secrecy outages are developed. Optimization problems are posed, and simulations validate the results. In [37], improving post-disaster surveillance using UAVs and CRN focuses on optimizing transmission power and data rate while addressing interference. Proposed algorithms exceed random power selection for higher data rates. In [38], utilizing a multi-agent reinforcement learning framework to enhance channel allocation in cognitive UAVs. Using UCB-H and DDQN, it shows improved network performance. In [39], a cognitive IoT system makes use of UAVs equipped with energy harvesting capabilities to act as relays, enhancing communication between a satellite source and IoT devices. A multi-objective optimization framework with the Outer Approximation Algorithm outperforms NOMAD. In [40], an energy-efficient UAV-based cognitive radio network that adjusts transmission power based on primary user sensing and energy harvesting using compound Poisson distribution. Optimized resource allocation is achieved with Lagrange duality, resulting in significant energy efficiency gains. In [41], the swapping method optimizes UAV deployment in disaster operations, improving connectivity, coverage, and network lifespan in high-pressure situations.

3. PROPOSED DICOT-CUAV MODELS

3.1 UAV-CRN NETWORK MODEL

This paper delves into an EH-UAV-CRN comprising a secondary network (SN) and a primary network (PN), which includes a pair of transmitters and receivers. The SN possesses a flying UAV known as ST, along with a designated receiver named SR. The SN can use PN's licensed spectrum for transmitting data. The user's location is conveniently represented through a three-dimensional Cartesian coordinate system. The aircraft ST navigates smoothly in a circular path at a height of H, maintaining a radius of R with its center positioned at $x_{ST}^{(0)}, y_{ST}^{(0)}, H$. Flight speed is represented by the symbol V, and the position of ST can be determined at any given time t. The angle of flight for ST is symbolized as $\frac{vt}{R}$. We can infer that PT is located at (x_{PT}, y_{PT}, 0) and PR is positioned at (x_{PR}, y_{PR}, *0*). Moreover, we can also presume that SR remains stationary at coordinates (x_{SR}, y_{SR}, *0*). Consequently, the distances from ST to SR and from ST to PR can

$$\left(x_{ST}^{(t)}, y_{ST}^{(t)}, H\right) = \left(x_{ST}^{(0)} + Rcos\left(\frac{vt}{R}\right)\right), \left(y_{ST}^{(0)} + Rsin\left(\frac{vt}{R}\right), H\right) \quad (1)$$

$$\mathrm{D}_{\mathrm{Pv}}^{(\mathrm{t})} = \sqrt{\left(x_{ST}^{(t)} - x_{SR}\right)^2 + \left(y_{ST}^{(t)} - y_{SR}\right)^2} + H^2 \quad (2)$$

$$\mathrm{D}_{\mathrm{SP}}^{(\mathrm{t})} = \sqrt{\left(x_{ST}^{(t)} - x_{PR}\right)^2 + \left(y_{ST}^{(t)} - y_{PR}\right)^2} + H^2 \quad (3)$$

In the same way, the distances for the connections between ST-PT and PT-SR can be outlined as follows.

$$\mathrm{D}_{\mathrm{PV}}^{(\mathrm{t})} = \sqrt{\left(x_{ST}^{(t)} - x_{PT}\right)^2 + \left(y_{ST}^{(t)} - y_{PT}\right)^2} + H^2 \quad (4)$$

$$D_{ps} = \sqrt{\left(x_{PT} - s_{SR}\right)^2 + \left(y_{PT} - y_{SR}\right)^2} \quad (5)$$

In the Figure 2. The UAV in CRN employs the standard frame design with each time slot comprising a sensing period τ and a transmission sub-slot T−τ. It should be noted that in this study, a frame refers to the duration of one UAV flight. Therefore, the duration of one frame can be expressed as

$$T = \frac{2\pi R}{v} \quad (6)$$

Initially, the UAV detects the condition of the primary transmitter (PT) during the sensing period and then establishes communication with the secondary receiver (SR) in the transmission sub-slot. The suggested approach involves integrating UAVs into cognitive radio networks (CRN) to facilitate operations in diverse scenarios. For instance, UAVs could be utilized for environmental monitoring by gathering data from ground nodes and relaying it to control centers or other UAVs for seamless communication. The channel gains denoted as $\tilde{g}_{pv}, \tilde{g}_{ss}, \tilde{g}_{sp}$ *and* $\tilde{g}_{ps}$ represent PT-ST, ST-SR, ST-PR, and PT-SR connections, respectively. To streamline the processing, we view each frame as representing a shading state. Considering the influence of weather and various unpredictable elements on the communication quality of a UAV, we investigate its communication performance under prolonged fading conditions. During a shading state, all connected links undergo block fading, where the channel state stays constant within a frame but switches between frames. The LOS links, specifically ST-PR, ST-PT, and ST-SR, are represented by a blend of small-scale fading and propagation loss in their modeling.

$$\tilde{g}_x = |g_x| \sqrt{\frac{\rho_o}{D_x^2}} \tag{7}$$

Consider x as a collection containing *pv*, *ss* and *sp*. The variable $|g_x|$ is established as a complex Gaussian random variable with an average value of zero and a variance of one. This variable considers the differences in signal strength between the main node (ST) and all the other nodes located on the ground. The symbol ρ_0 denotes signal attenuation for every unit of distance, and the expression $\sqrt{\frac{\rho_0}{D_x^2}}$ demonstrates how much path propagation is influenced by the Euclidean distance separating ST and ground nodes as per equations 2–4. The remaining ground-to-ground channels exhibit characteristics of Rayleigh fading. Within this context, the symbol α signifies the factor that describes the attenuation of signal intensity as distance increases, while g_{ps} denotes the variations in signal strength caused by sudden environmental changes. The direct distance between the transmitter and receiver is referred to as D_{ps} in a point-to-point link. Moreover, it is understood that the primary user's signals are characterized by complex phase-shift keying (PSK), whereas the noise received by the secondary receiver is circularly symmetric, following a Gaussian distribution with zero mean and unit variance. Spectrum sensing refers to the process of identifying the frequencies that are currently accessible. When a UAV has access to the same spectrum as a primary user (PU), there may be interference if both users are present. To avoid this, the secondary user (ST) needs to sense the spectrum and determine when it is safe to use the authorized band. Where the UAV uses an energy detection (ED) method to assess the presence of a PU, resulting in a binary hypothesis test.

The value of n represents the n-th sample of PT's signal, while $y(n)$ represents the signals received by the UAV. The signal sent by PT is denoted as $s(n)$, and the n-th noise sample is represented as $v(n)$. The spectrum sensing result using energy detection (ED) is expressed as $T(y) = \frac{1}{fs^{\tau}} \sum_{n=1}^{fs^{\tau}} |y(n)|^2$, where fs is the sample frequency. It is important to point out that since the connection between ST and PT is a dependable line-of-sight (LoS) link, any possible fading effects on the UAV's sensing decisions can be disregarded. Hence, when employing an ED strategy, the calculation of detection probability and false alarm probability can be done in the following manner.

$$P_d(\tau, \varepsilon) = Q\left(\left(\frac{\varepsilon}{N_0} - \gamma - 1\right)\sqrt{\frac{\tau f_s}{2\gamma + 1}}\right) \tag{8}$$

$$P_f(\tau, \varepsilon) = Q\left(\left(\frac{\varepsilon}{N_0} - 1\right)\sqrt{\tau f_s}\right) \tag{9}$$

In this situation, the symbol ε signifies the minimum detectable level of Emergency Department (ED) detection, while γ represents the ratio of signal strength to noise received by the UAV. Q(·) is the inverse of the standard Gaussian distribution function, symbolized as $\frac{1}{\sqrt{2\pi}} \int_0^u \exp(-t^2/2) dt$. Additionally, a predetermined threshold $\bar{P}_d$ is set to ensure complete protection of the primary user from interference. As a result, $P_f(\tau, \varepsilon)$ can be reevaluated using this information. In the allocated time for transmission, the UAV can regulate its transmission strength based on its sensing results. This means that when the primary user (PU) is not in use, the UAV will transmit with greater power, denoted as $P_s^{(0)}$, while it will use lower power, denoted as $P_s^{(1)}$, if the PU is detected as occupied. By doing so, the UAV can efficiently utilize the licensed spectrum and prevent any major interference with the PU. However, due to limitations in spectrum sensing technology, such as shadowing and fading, there may be errors in the sensing process. As a result, there are four possible scenarios depending on the sensing results and status of the PU. The primary user (PU) is not in use and the unmanned aerial vehicle (UAV) can detect it correctly with a probability of a_0, which is equal to the probability of the PU being inactive H_0 multiplied by the probability of false detection P_f. The SU's rate at that moment is $r_{00} = log_2\left(1 + \frac{\tilde{g}_{ss} P_s^{(0)}}{N_0}\right)$. The primary user's status is currently inactive; however, the unmanned aerial vehicle

incorrectly detects it as busy with a chance of $a_1 = P(H_0)$ P_f. Furthermore, the current data rate of the secondary user is $r_{01} = log_2\left(1+\frac{\tilde{g}_{ss}P_s^{(1)}}{N_0}\right)$. The primary user is currently occupied, however, there is a possibility that the unmanned aerial vehicle may falsely detect it with a probability of β_0, which is equal to the probability of the primary user being present $P(H_1)$ multiplied by the probability of detection $(1 - P_d)$. The SU's instantaneous rate can be represented as $r_{10} = log_2\left(1+\frac{\tilde{g}_{ss}P_s^{(0)}}{P_p g_{ps}+N_0}\right)$. The primary user is occupied and the unmanned aerial vehicle correctly identifies this with a probability of $\beta_1 = P(H_1)P_d$. The current speed of the secondary user is $r_{11} = log_2\left(1+\frac{\tilde{g}_{g}P_s^{(1)}}{P_p g_{ps}+N_0}\right)$. In this context, $P(H_0)$ refers to the likelihood of the primary user (PU) being idle, while $P(H_1)$ represents the probability of the PU being busy. The initial number in the instantaneous rate indicates the actual state of the PU (0: available; 1: occupied), while the second number shows the detection outcome by the unmanned aerial vehicle (UAV) (0: not present; 1: present).

3.2 UAV DATA TRANSMISSION

This section of the text details the creation and design journey for the Decision-based Routing for Unmanned Aerial Vehicles and the Internet of Things (DR-UAV IoT) routing solution, which is crafted upon distinct decision criteria. The solution involves two primary phases: directing data between UAV nodes and transmitting data from UAVs to IoT infrastructure devices. It functions as a tool for determining how data should be routed, especially when the ground network is crowded and unable to send data to the decision center or main servers. The IoT infrastructure is responsible for gathering and transmitting data to UAV nodes, which subsequently relay it to cloud or backbone devices to enhance decision-making processes. The development of the two primary modules in this solution was carefully crafted through a series of steps. The initial module emphasizes UAV-to-UAV communication, facilitating data routing among UAV nodes. On the flip side, the second module leverages the proposed solution to collect data from base stations (BS) and integrate it with the IoT network situated on the ground. Usually, BS is well-equipped with ample resources such as bandwidth, transmission power, and coverage. This module makes use of location services for communication between nodes. These services strive to acquire precise and current node locations. Moreover, the DR-UAV IoT system utilizes location services to enhance the functionality of IoT network services. UAV nodes are present in the network to support IoT networks, whether in densely populated or sparsely populated network environments. Over time, this solution accurately assesses ground network density by measuring distances among UAV nodes and pinpointing areas with heavy traffic through the exchange of brief messages. Furthermore, battery power levels are also checked by UAVs before participating in data collection activities; priority is given to drones with ample battery power. Figure 1 illustrates the components of a drone.

The control station, also known as the BS, plays a crucial role in managing IoT and UAV traffic. Its main function is to support the network and enable strong transmission and receiving capabilities. This can be a difficult task as UAVs and IoT nodes often face challenges in communication due to limited ad hoc networks. The BS helps overcome these limitations by providing support to enhance the network and adjust channel conditions and paths for UAVs and nodes. However, data collection can still be a challenge if the BS does not meet network requirements. In order to reduce interference, every base station function on a designated frequency, with its communication coverage dictated by the size of the cell. Furthermore, the Base Station is connected to a central entity called the mobile telecommunication switching office to facilitate additional data analysis. In this section, we utilize the suggested routing approach for the transmission of data. The module is structured around two primary phases: UAV-to-IoT and UAV-to-UAV data routing. During the initial phase, data is gathered from IoT networks on the ground, with the nodes' positions being pinpointed through GPS technology. The UAV employs a routing strategy to pinpoint a designated area, like a stadium, field, or disaster site, by utilizing up-to-date data on node density in the ground IoT network. This is accomplished by the innovative DR-UAV IoT protocol, which initially collects data on node density from a centralized IoT infrastructure. Next, every UAV node identifies the connectivity factor and chooses the appropriate region for data gathering. In order to assess node density, the solution employs pre-segmented fixed zones that have a communication range of 250 meters. Every UAV node ensures full coverage of its assigned area while keeping data up-to-date through the exchange of Hello packets with IoT nodes located on the ground. This guarantees that each UAV node possesses a current routing table that relies on details regarding node density. Figure 2 showcases the exchange of Hello packets happening at ground level.

The UAV updates the routing table by recording the number of nodes and their corresponding locations within the designated zone. Equation (1) demonstrates the calculation of the total number of IoT nodes in the selected area.

$$IoT_{Node}(Total_{Zones}) = \sum_{i=1}^{|Total_{Zones}|} IoT_{Node}(Area) \quad (10)$$

The $|Total_{Zones}|$ signify the total number of zones in a particular region, while the $IoT_{Node}(Area)$ refers to the

Figure 1. Essential parts of a drone

quantity of nodes existing in the IoT network. Moreover, the level of connectivity plays a vital role in the proposed protocol, established through the analysis of density data collected from the BS. The UAV nodes make use of the density table to evaluate the connectivity level and calculate it accordingly. This table presents data on node density obtained from the information collected by the BS.

Figure 2. Estimating the density of IoT Network Nodes using Unmanned Aerial Vehicles (UAVs)

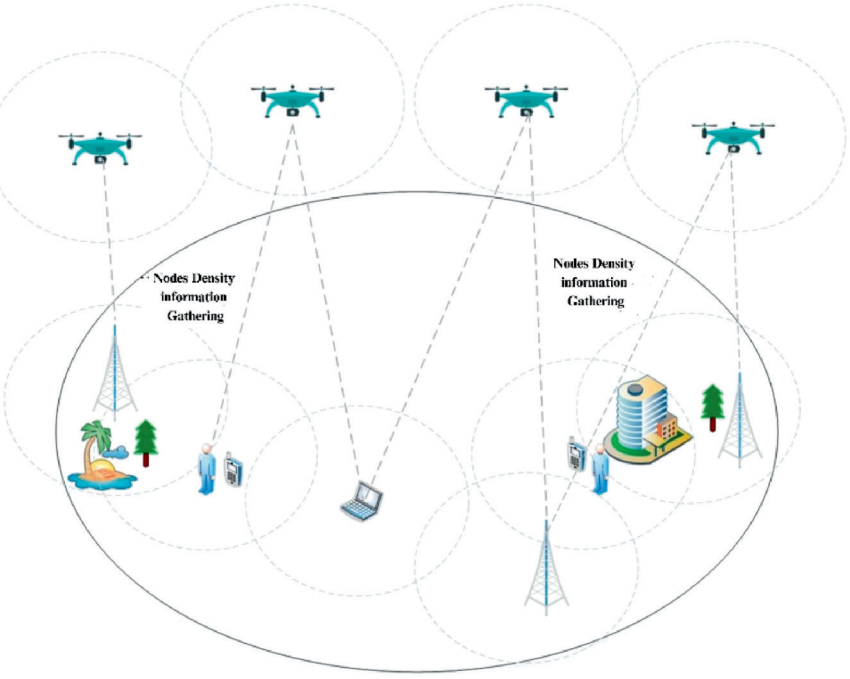

Figure 3. The communication distance of every element within the network

The DR-DR-UAV IoT protocol's design depends on the BS for connectivity and as a key infrastructure for providing services. Figure 3 provides a visual representation of the communication flow among the Base Station, UAVs, and IoT nodes. The BS degree plays a vital role in supporting data communication within IoT networks that rely on various communication technologies and standards. Its primary role is to offer communication services to both IoT nodes and UAV nodes. The Bright Star is fully furnished with essential resources like batteries, processing units, storage devices, and robust long-range receiver and transmission tools. We make use of GSM IoT (EC-GSM-IoT) services to send data, as it effectively saves energy and enables long-range communication for IoT devices, serving as a low-power wide area network technology. Numerous studies have shown how effective GSM IoT service is when compared to alternative standards such as Wi-Fi and cellular networks. The transmission range and coverage area of UAVs depends on the density of nodes present on the ground. Additional transmission power is needed for nodes in an IoT network with more nodes than UAVs to facilitate data sensing and collection, while microcells support the transmission power requirements for UAVs. Algorithm 1 details the steps involved in linking UAVs to an IoT network.

The beginning of the UAV-to-UAV data communication process occurs during the second module. This entails the exchange of information among the drones' nodes to monitor ground updates and status. In this phase, a responsive routing strategy is utilized, allowing the protocol to create routing paths as required. The primary goal of this module is to identify nearby and nearest UAV nodes for seamless connectivity. Nevertheless, the network cannot

Algorithm 1. (UAV-to-IoT)

Input: CUAV: The potential unmanned aerial vehicle (UAV) point
Output: The density of nods in IoT network

1. IoT: Internet of Things network point
2. If (Data on traffic density is received from the IoT network through a base station)
3. Then (Establish coordinates using location service) Else
4. Transmit broadcast messages to assess the node density within the IoT network.
5. If congestion is identified within the IoT network.
6. Gather information from the IoT network.
7. Alternatively, wait for a random interval before repeating the procedure.
8. End task
9. Find out the distance and then travel to the designated destination.
10. End if
11. End process

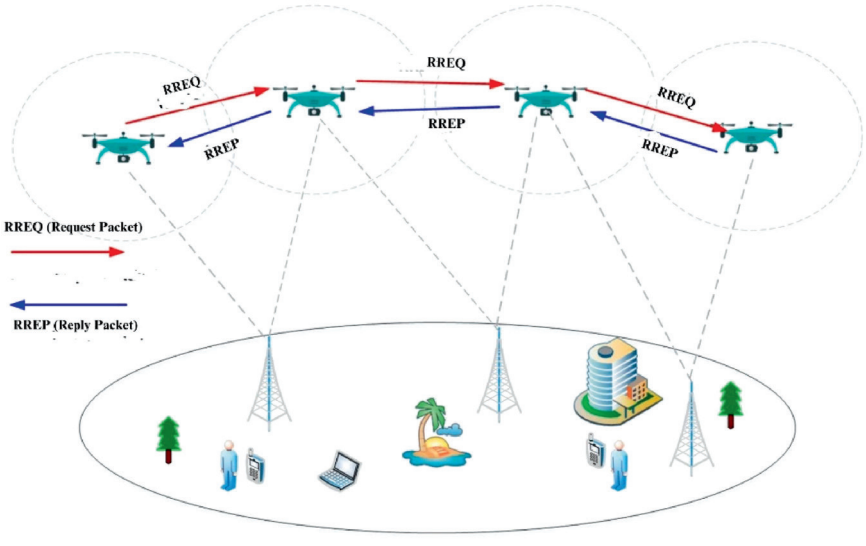

Figure 4. The procedure for sending route reply messages between unmanned aerial vehicles (UAVs) is known as the RREP process

Algorithm 2. Outlines how data communication occurs among UAV-to-UAV nodes using RREQ packets

Input: communication between UAVs
Output: to achieve the destination of RREQ

1. Begin by initializing the process.
2. Designate a UAV node as the candidate (CUAV).
3. Create a Route Request Packet (RREQ).
4. If the UAV receiving the RREQ is the same as the CUAV, disregard the request.
5. Otherwise, proceed to step 6.
6. If the destination of the RREQ is the same as the CUAV, select a route.
7. Otherwise, wait for a random time and repeat the process.
8. Record that the RREQ was received by the CUAV.
9. Add the RREQ to be rebroadcasted later.
10. Rebroadcast the RREQ to other UAVs.
11. End the if process.
12. End of process flow.

ensure uninterrupted data transmission due to the frequent disconnections caused by the high mobility of UAVs. The suggested DR-UAV IoT protocol effectively tackles this concern by enabling decisions and exploring alternative pathways without the need to restart the discovery process. In order to establish a connection smoothly, the UAV node initiates by updating its routing table to include details regarding the locations of the source (IoT nodes) and destination (Main Center devices). Subsequently, by utilizing additional interconnected UAV nodes in the sky, a routing path is established towards the intended destination to efficiently relay data. The Route Request Packet (RREP) is utilized to keep this route updated. After gathering all data from IoT nodes, it is then seamlessly transmitted to the central hub, strategically positioned according to network specifications. For example, in a sports stadium setting, the central command would typically be in the control room. The RREP packets consistently seek direct link nodes for transmitting data packets. Figure 4 showcases the RREP process between UAV-to-UAV nodes.

The RREQ packet includes important information such as the identification numbers of the source and destination UAVs, a unique RREQ ID, and data regarding the latitude and altitude of the UAV. To avoid network overload, a suggested approach includes combining the use of UAV-ID with an RREW message. If the UAV node receives the same identification number, it will ignore it. The route reply (RREP) messages are later dispatched from the immediate UAV node to acknowledge receipt to the source UAV node. Subsequently, a routing decision is reached as nodes share route information for a predetermined duration. Once this period elapses, all RREQ messages will be discarded.

3.3 CHANNEL MODEL

The location of the UAVs is given by X_m, Y_m, H_m, while the IoT device is represented by (x_i, y_i, 0). This means that the distance between them can be calculated as

$$d_{\text{im}} = \sqrt{(X_m - X_i)^2 + (Y_m - Y_i)^2} \tag{11}$$

Each minor affected region is thought to be monitored by a single drone that operates within the specified service range assigned to it. If the IoT device sends a task to drone M, it needs to be positioned within the drone's coverage area. The UAV's maximum coverage radius is established by the parameter d_{max}. Communication between the IoT device and drone takes place wirelessly. To prevent any disruption, IoT devices utilize FDMA to offload computing tasks onto drones. When an IoT device and drone are communicating, the drone will fly near the ground, ensuring a direct line of sight with minimal signal interference. The data rate for the uplink can be determined by the variable r. The channel bandwidth between the IoT device and the UAV is denoted as ω_u, with $g_{i,m}$ representing the uplink channel gain. The symbol σ^2 indicates the strength of additive white Gaussian noise (AWGN), while pi stands for the transmission power of the channel. The term g_0 denotes the channel gain of the reference channel, whereas $d_{i,m}^2 + H_m^2$ signifies the Squared Euclidean Distance from the IoT device to the UAV. The distance separating the UAV and LEO satellite enables the satellite to access the communication window only when α reaches 20 or above, without factoring in any other influences. The positions of the UAVs are designated as X_j, Y_j, H_j. The geocentric angle θ_{mj} measures the angle between Earth-based IoT devices and satellites. The Earth's radius is symbolized as R, with the UAV's height indicated by H_m. The satellite's altitude is represented by H_j and α represents the horizontal angle between the UAV and the satellite. The peak value of the communication window θ is achieved at α being 20. To determine the distance, you can use the following calculation method.

$$\theta_{mj} = \arccos\left(\frac{R + H_m}{R + H_j}\cos\alpha_j\right) - \alpha_j \tag{12}$$

$$H_{mj} = \sqrt{(R+H_m)^2 + (R+H_m)^2 - 2R(R+H_m)cos\theta_{mj}} \quad (13)$$

As stated in 3GPP Release15, an extra change in frequency caused by the movement of satellites must be considered by using the following equation:

$$f_{j,m} = \left(\frac{v_{sat}}{C}\right) \times \left(\frac{R+H_m}{R+H_j} cos\alpha\right) \times f_{m,j} \quad (14)$$

The velocity of the satellite is denoted as v_{sat}, while c represents the speed of light, and $f_{m,j}$ symbolizes the carrier frequency at the transmitter. The formula calculates the transmitting gain of the drone antenna and the receiving antenna gain of the satellite. The performance level of the antenna is denoted by φ, where Ω_m and Ω_j are the dimensions of the antennas on the reflecting surfaces of the UAV and satellite, respectively. The symbol 'c' represents the speed of light. The channel coefficient pertaining to the UAV-LEO channel. The variables u_{mj} and l_{mj} represent the path loss factor. More precisely, the formula for path loss factor is denoted as $u_{mj} = \left(\frac{4\pi H_{m,j}}{\lambda_{m,j}}\right)$, in which $\lambda_{m,j} = c/f_{m,j}$.

The data rate of the uplink channel can be determined using the Shannon formula, with Q denoting the Rician fading factor. The symbol $|\overline{l}_{m,j}|$ denotes the line-of-sight (LoS) element having a value of 1, while $\overline{l}_{m,j}$ signifies the non-line-of-sight (NLOS) component, which adheres to a sophisticated Gaussian distribution with an average of 0 and a variability of 1. B indicates the frequency range used to establish the connection between the UAV and the satellite, $P_{m,j}$ represents the transmission power of the UAV's uplink, and N_0 denotes the spectral density of noise power.

3.4 DATA OFFLOADING AND COMPUTING

The ground equipment transfers the task to the UAV, which then delivers the task block S_i through the UAV to leo_j for processing. a_{ij} = 1 is used to show that leo_j can process the task, while vice versa indicates that the task S_i is not given to leo_j for processing. The time it takes for an IoT device to transfer the task S_i to a UAV through the channel involves two types of delay: transmission and propagation. These delays denoted as T_{im}^{tran} and T_{im}^{prop}, respectively, can be calculated using the equation.

$$T_{im}^{tran} = \frac{s_i}{r_{im}}, \; T_{im}^{prop} = \frac{d_{im}}{c} \quad (15)$$

The speed of light is represented by the variable c. This formula can be used to express the time difference between the IoT device and the drone.

$$T_{im} = T_{im}^{tran} + T_{im}^{prop} \quad (16)$$

The amount of energy used by the device to communicate with the drone is computed as.

$$E_{im} = \omega_u T_{im} \quad (17)$$

In the communication path between the UAV and LEO, the time it takes to transfer task S_i from the UAV to leo_j consists of three components: transmission delay T_{im}^{tran}, propagation delay T_{im}^{prop}, and computation delay T_J. These can be described individually as follows.

$$T_{mj}^{tran} = \frac{S_{ij}}{R_{mj}}, \; T_{mj}^{prop} = \frac{H_{mj}}{c}, \; T_j = \frac{S_{ij}\beta}{f_{ij}} \quad (18)$$

Task volume size transferred represented by S_{ij}, the Central Processing Unit requires β cycles to finish processing one unit of the task volume, while f_{ij} reflects the computation frequency allocated to S_{ij} by leo_j.

$$T_{mj} = T_{mj}^{tran} + T_{mj}^{prop} + T_j \quad (19)$$

The transfer of task volume from S_{ij} to leo_j is denoted by S_{ij}, while the CPU requires β process cycles to execute a single bit of this volume. Additionally, f_{ij} denotes the computing frequency allocated by leo_j for S_{ij}. The delay between the drone and the satellite is represented by S_{ij}. The energy consumption is comprised of two components: the energy required for transmitting data and the energy necessary for computing on the LEO satellite. The transfer energy consumption is determined by the equation.

$$E_{mj} = \frac{P_{mj}S_{ij}}{R_{mj}} \quad (20)$$

$$E_j = kS_{ij}\beta f_{ij}^2 \quad (21)$$

$$T = T_{prop} + T_{tran} + T_j, E = E_{im} + E_{mj} + E_j \quad (22)$$

The satellite's energy consumption is established based on the uplink power of UAV m, which is represented as $P_{m,j}$ in the equation provided. The energy factor, denoted as k, governs both the overall time delay (T) and complete energy consumption (E). T_{prop}, or the overall delay in propagation time is determined by adding together the individual propagation delays $T_{prop} = T_{im}^{tran} + T_{im}^{prop}$. Similarly, T_{tran} represents the total delay in transmission time, which can be calculated by combining the individual transmission delays $T_{tran} = T_{im}^{trans} + T_{mj}^{trans}$.

3.5 UAV OPERATIONS

The unmanned aerial vehicle effortlessly holds a consistent altitude referred to as z during its flight.

In practical scenarios, the height is typically adjusted to the lowest feasible level to navigate around obstacles like buildings and trees effortlessly, minimizing the need for frequent adjustments in vertical positioning. The UAV's responsibilities can be divided into three main categories: movement, data transfer, and wireless power distribution. This implies that the controller directs the UAV to perform these operations during every time interval. UAV can either remain stationary or move to a nearby location using energies respectively. At the same time, there is a designated charging station for the UAV located at LC. Staying within close range of this charging location allows for frequent recharging of the UAV, ensuring it has enough energy to continue its tasks. The scenario poses a challenge for sensor nodes (SNs) situated at a distance from the charging station. In these situations, the SNs are unable to receive support from the UAV as they are unable to transmit collected data or be charged by it. This may lead to reduced lifespans for SNs and insufficient gathering of data. In order to tackle this concern, it is important for decisions regarding the UAV's movement to take into account not only its energy levels but also those of the SNs.

The UAV acts as a bridge between the SNs and GW, enabling the merging of data. If the transmission of data to the GW directly upon receiving it from the SNs were to occur immediately, the device's energy would rapidly diminish. To prevent this, the UAV can combine data and delay transmission to the GW until it has accumulated a certain amount of data or is within proximity to the GW. This allows for simultaneous delivery of data in a single packet. However, excessive aggregation may result in obsolete data if the service update cycle ends before transmission to the GW. When making decisions about transmission operations, it is important to consider both the energy levels of the UAV and the service update cycle. For the efficient transfer of wireless power, it is presumed that the UAV employs a directional antenna set at a fixed angle. This implies that energy from the UAV can only be received by SNs positioned in matching locations on the ground plane with a location in the UAV plane. The energy consumption of the power transfer, denoted as , is not required for Sensor Nodes (SNs) having ample energy reserves. Moreover, should the UAV find itself distant from its charging site and rely too heavily on wireless power transfer, it could face difficulty returning as a result of energy exhaustion. Hence, when making decisions about wireless power transfer, one should consider the UAV's current location and the energy levels of both the UAV and the SNs. The following section introduces a sophisticated Deep UAV algorithm, crafted to enhance movement, data transmission, and wireless power transfer all at once. In this algorithm, the controller consistently enhances the UAV's operations through online training, refining its policies via a process of trial-and-error learning. This is accomplished by integrating observational data from the state and experiential knowledge into a nonlinear function approximator, more precisely, a neural network. The neural network undergoes iterative training to equip the controller with nearly optimal decisions for every state.

3.6 THROUGHPUT AWARE OPTIMIZATION

The Whale Optimization Algorithm (WOA) emerged in 2016, drawing inspiration from the hunting techniques employed by humpback whales. This approach is designed to replicate the method used by humpback whales as they surround and follow their prey. The whales follow a two-stage process in their hunting activities, beginning with exploration and then moving on to exploitation. In the same manner, the WOA algorithm functions through two phases to navigate the search space effectively to find the best solutions. In the exploration stage, the algorithm sets its sights on the current best solution as its target prey. As the optimal solution is not known initially, the algorithm first considers the current leading candidate

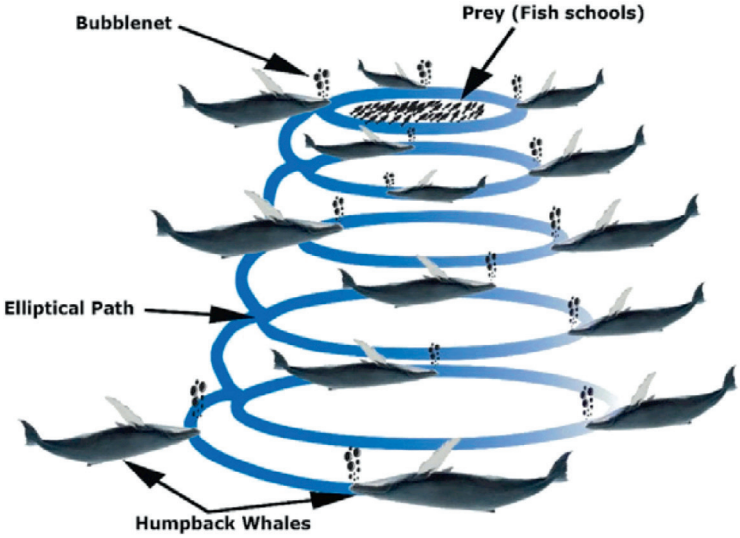

Figure 5. The act of bubble-net feeding performed by humpback whales

as the target and then directs other possible solutions represented as "whales" to modify their positions in the search space accordingly. Figure 5 beautifully illustrates the cooperative hunting technique of whales, commonly referred to as bubble-net feeding. Whales employ circular or "9"-shaped movements, releasing bubbles to assist their hunting maneuvers in this strategy. Further exploration of this behavior has revealed its capability to mimic problem-solving in optimization. The simulation explores the use of group searching, encircling, and pursuit techniques within a community of whales, offering valuable perspectives on innovative optimization strategies.

If we consider a group of N whales in a search area defined by D dimensions, the location of each whale can be denoted as $X_i = (X_{i,l}, X_{i,2}, \ldots, X_{i,D})$, where i represents their specific position in the group. When it comes to optimization, the whales are aiming to encircle their desired target prey by assessing the current best position within the group. This encourages them to shift their stances toward the optimal solution. This behavior assists in encircling the prey, and certain whales may also approach the most skilled individual for additional refinement. The repositioning process is directed by specific equations known as Eqs. Whales are prompted to gradually approach the target prey or the most suitable individual for encircling it in actions (23) and (24). The equations illustrate how the algorithm operates, showing how the whales navigate the search space to discover the most efficient solutions. The equations probably illustrate how solutions (UAV fog node coordinates) or "whales" adjust their positions around a hypothesized ideal solution, reflecting the algorithm's process of both exploring and exploiting to discover the best placement for UAVs. The vector $\vec{D}$ represents the difference between the product of vector $\vec{C}$ and the most successful solution obtained at the current time ($\vec{X}*$), and the current solution $\vec{X}(t)$ and $\vec{X}(t+1)$. It then refines the current solution based on D, adjusting it towards the optimal solution ($\vec{X}*$) at time t by applying coefficient vectors A and C. These coefficients are derived from specific equations (25) and (26) that incorporate vectors $\vec{a}$ and $\vec{r}$. The calculation of $\vec{A}$ and $\vec{C}$ is determined by these equations.

$$\vec{D} = \left|\vec{C}.\left(\vec{X}*\right)(t) - \vec{X}(t)\right| \tag{23}$$

$$\vec{X}(t+1) = \left(\vec{X}*\right)(t) - \vec{A}.\vec{D} \tag{24}$$

$$\vec{A} = 2\vec{a}.\vec{r} - \vec{a} \tag{25}$$

$$\vec{C} = 2.\vec{r} \tag{26}$$

The vector $\vec{a}$, gradually decreasing from 2 to 0 throughout iterations, holds significant importance in maintaining a balance between exploration and exploitation in the optimization process. In the same way, the random vector $\vec{r}$, where values fall between 0 and 1, brings a touch of unpredictability to the Whale Optimization Algorithm. The element of randomness allows every search agent, depicted as a solution, to navigate through various positions across the search space. This investigation helps prevent the algorithm from becoming trapped in local optima, enabling a wider array of potential outcomes. Therefore, the relationship between vector $\vec{a}$ and $\vec{r}$ vector has a significant impact on both exploration and exploitation throughout the optimization process. Additionally, WOA incorporates two foraging techniques inspired by humpback whales to facilitate the exploration of the best solutions. The Shrinking Encircling Mechanism draws inspiration from the bubble net technique famously employed by humpback whales and plays a pivotal role in the strategy of the WOA. The primary goal of this algorithm is to reduce the coefficient vector $\vec{A}$ by lowering the value of $\vec{a}$ (as demonstrated in Equation. 25 could you please rephrase the previous information smoothly. During

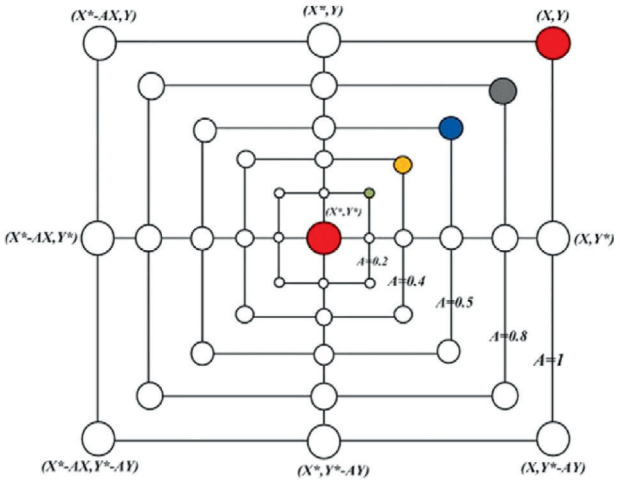

Figure 6. The most effective solution currently achieved is the Bubble-net search method (X*)

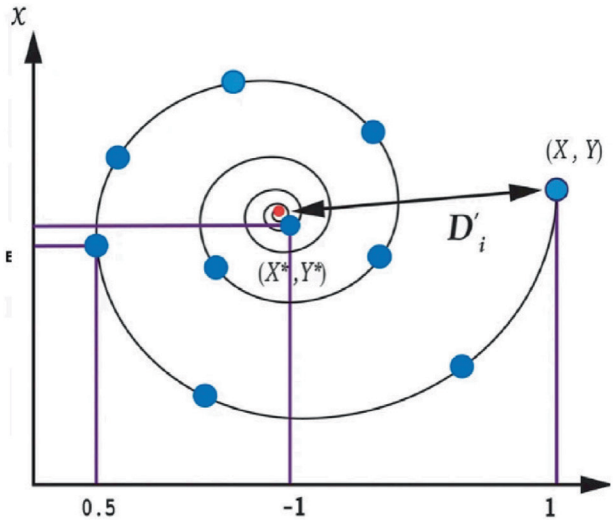

Figure 7. The position is being updated in a spiral pattern

this procedure, search agents adapt their positions towards a new location by striking a balance between their initial position and the most effective solution at present. This method emulates the concept of strategically surrounding and focusing on a promising solution. In the figure 6, we are presented with a visual representation illustrating the possible locations of a search agent as it moves from its starting coordinates (X,Y) to a fresh position (X',Y'). This illustration clearly shows how the agent's position changes over iterations within a specific parameter space, influenced by both the shrinking of vector a and random values of vector $\vec{A}$.

The algorithm utilizes a spiral motion to imitate the movement of humpback whales while foraging. The distance between the whales and the location of their prey, denoted as vector $(\vec{D})$, needs to be determined. The calculation of (27) is done to establish their location. By employing a spiral equation with variables such as b, influencing the spiral's shape, and a random number l, the agents' positions are smoothly adjusted along a path that elegantly traces a spiral pattern bridging their present whereabouts and the most optimal solution discovered thus far. This approach replicates the effective way whales navigate through search areas. The image depicted in the figure. In the seventh section, it is illustrated how this

Algorithm 3. WOA

Input: The best search agent X* from a population of whales Xi (where i = 1,2,...,n)
Output: to Calculate fitness for a search agent

1. Begin by establishing the population of whales.
2. Evaluate the fitness of every search agent.
3. The best search agent is represented by X*.
4. If the number of iterations remains below the maximum limit.
5. For each search agent:
6. Update parameters *a, A, C, l, and p*.
7. If p is less than 0.5:
8. If 2 multiplied by the absolute value of A is less than 1:
9. Update the position of the current search agent using $\vec{D} = \left|\vec{C}.(\vec{X}*)(t) - \vec{X}(t)\right|$
10. End if statement.
11. Else if 2 multiplied by the absolute value of A is greater than or equal to I:
12. Select a random search agent X_{rand}.
13. Update the position of the current search agent using $\vec{D} = \left|\vec{C}.(\vec{X}_{rand}) - \vec{X}\right|$.
14. End if statement.
15. End else statement.
16. Else if p is greater than or equal to 0.5:
17. Update the position of the current search agent using $\vec{X}(t+1) = \vec{D} \cdot e^{bl} \cdot \cos(2\pi l) + \vec{X}*(t)$.
18. End if statement.
19. End else statement.
20. Verify whether any search agent has exceeded the search boundaries and make necessary adjustments to its position.
21. Determine the fitness level of every search agent.
22. If a more suitable solution is found, please make the necessary updates to X.
23. Increment iteration counter t by 1.
24. Return X* as the best solution found so far.
25. End algorithm.

approach influences the way whales navigate around their prey. Their location gradually shifts using a probabilistic selection between two updating strategies: shrinking circles and spiral movement.

$$\vec{X}(t+1) = \vec{D} \cdot e^{b1} \cdot \cos(2\pi l) + \vec{X} * (t) \quad (27)$$

Equation 28 employs probability-based selection to determine whether to use the mechanism is either referred to as the Shrinking Encircling Mechanism or the Spiral Updating Position and is structured in the following way:.

$$\vec{X}(t+1) = \begin{cases} \vec{X} * (t) - \vec{A} \cdot \vec{D} \text{ if } p < 0.5 \\ \vec{D} \cdot e^{b1} \cdot \cos(2\pi l) + \vec{X} * (t) \text{ if } p \geq 0.5 \end{cases} \quad (28)$$

$$\vec{D} = \left| \vec{C} \cdot (\vec{X}_{rand}) - \vec{X} \right| \quad (29)$$

$$\vec{X}(t+1) = (\vec{X}_{rand}) - \vec{A}.\vec{D} \quad (30)$$

The vector $\vec{A}$ plays a crucial role in guiding the exploration phase of the Whale Optimization Algorithm (WOA). If magnitude of vector $\vec{A}$ exceeds 1, it suggests that the algorithm is primarily inclined towards exploration. This phase focuses on refreshing the positions of the remaining search agents by considering the top solution discovered until now. Consequently, these search agents heavily depend on information obtained from the current best solution to direct their exploration within the search space. Therefore, the threshold of vector A plays a pivotal role in the algorithm by determining its exploration phase. It guarantees that once vector $\vec{A}$ surpasses this limit, the emphasis remains on exploration. This guides the search agents to explore the search space effectively, drawing insights from the current optimal solution. Equations (29) and (30) embody a critical mathematical model that describes an exploration strategy in WOA. The vector $\vec{X}_{rand}$ symbolizes a solution chosen at random from the existing pool of potential solutions. In our current scenario, we harness the power of WOA to enhance the placement of UAV fog nodes. This process consists of several key stages. At first, a collective of whales is formed, where each whale symbolizes a prospective spot for a UAV fog node across the search region. These whales consistently venture into and utilize the search area, dedicating specific phases to each task. While exploring, whales choose the optimal current solution as their target prey and lead other whales to adapt their positions accordingly. During the exploitation phase, the whales elegantly circle their target prey, carefully selecting the best candidate for further refinement. Equations tailored for the Weighted Optimization Algorithm determine these position adjustments according to the exploration and exploitation phases. The process continues cycling until a specific termination condition is fulfilled, indicating that the best solution discovered signifies the most optimal arrangement of UAV fog nodes. To enhance clarity, a visual flowchart illustrating the optimization process has been provided for an easier understanding of the steps.

3.7 DYNAMIC INTELLIGENT CHANNEL ASSIGNMENT MODEL

In this section, we will describe a single cycle of the DICOT-CUAV protocol, in which the deployed SNs are grouped into clusters. A UAV leads each cluster, functioning as a CH. It gathers data from its CMs and transmits it to the BS. Throughout every cycle, UAVs reach designated positions above the Area of Interest at a set altitude to maximize coverage of as many Sensor Nodes as feasible. Before utilizing unlicensed spectrum, the UAVs conduct a Clear Channel Assessment (CCA) to verify that the channel is available. Upon successful completion of the CCA process, the UAV swiftly transmits *WuCs* to the ground SNs, thus commencing the cluster formation. After their formation, SNs within each cluster transition into becoming CMs dedicated to a particular UAV. This marks the commencement of the steady-state phase, during which data is gathered from the SNs on the ground. Once the data collection process is finished, CMs have the option to enter sleep mode, indicating the end of a single cycle. In the beginning stage, we will elucidate the process of cluster formation for a lone UAV in a single round, as illustrated in Figure 8. Since the clusters do not overlap and operate independently, the identical approach is applied to each formation. At the start of every round, all ground sensor nodes are in sleep mode, with their mobile relays turned off. Nevertheless, the *WuRx* consistently stays powered on, ready and waiting to receive a Wireless Command (*WuC*) from an UAV. When the SN's *WuRx* detects a *WuC* from an incoming UAV that has completed CCA successfully, its MR is activated, a process that requires some time referred to as the mode switching time (MST). The SN proceeds with CSMA-CA protocol before transmitting a joining request as a response to the targeted UAV's *WuC* signal. If several SNs receive the broadcasted *WuC*, each will attempt to send a separate joining request while they are in an active state. Nevertheless, collisions are bound to occur when transmitting these requests in reply to the *WuC*, as all SNs share channel access. To avoid collisions, we employ IEEE 802. 15. 4 non-beacon mode unslotted CSMA-CA to guarantee the successful transmission of joining requests from SNs to UAVs, as illustrated in the figure. It is crucial for the successful transmission of joining requests as this will determine if an SN will join in cluster formation. In unslotted non-beacon mode, CSMA-CA operates smoothly as each station gracefully adheres to a back-off algorithm. This involves patiently waiting for a random duration before assessing the channel's status. If the channel is unoccupied, the station can send its request to join. In case the channel is occupied, the station will increase its back-off counter and adjust the back-off exponent accordingly. The process keeps going until the station either reaches the maximum back-off attempts or successfully transmits

its request. The likelihood of channel occupancy following CCA, known as γ, plays a crucial role in analyzing the behavior of CSMA-CA. This can be computed through two mathematical models: *M/G/1 and M/G/1/2*. In this study, we employ the *M/G/1/2* framework to ascertain the likelihood of a station being unable to join a cluster and consequently being excluded from participating in cluster formation, as expressed by.

$$P_{drop} = \gamma^{mac\ MAXCSMA\ Backoffs+1} \tag{31}$$

The probability of an SN being dropped and unable to participate in the current cluster formation for the UAV round is represented by P_{drop}. The variable *macMAXCSMABackoffs* represents the limit for the number of CCA attempts allowed. In cases where an SN faces difficulty transmitting a join request, it enters a sleep mode to preserve energy. It is important to mention that the research does not cover the modeling of CSMA-CA. Concurrently with the CSMA-CA process, the station carefully readies data packets for sending. This procedure takes place at every SN in the Field of Interest (FoI), where it includes identifying *WuC via the SN's WuRx*, initiating the MR, generating data packets, executing CSMA-CA, and transmitting a request to join. The UAV gracefully accepts a connection request from every Sensor Node (SN). It then gracefully logs the Identity (ID) of each unique Sensor Node, marking them as Cluster Members (CMs) and allocating TDMA slots for their use. Consequently, a cluster is established where UAVs serve as Cluster Heads (CHs). This stage is commonly referred to as the setup phase, which is then succeeded by the steady-state phase. In the stable phase of DICOT-CUAV, a Sensor Node acting as a Cluster Member will receive a Time Division Multiple Access (TDMA) slot allocation from its Cluster Head, which is the Unmanned Aerial Vehicle (UAV). During this phase, the CM is tasked with transmitting its data packets within its allocated slot. After successfully sending the transmission, the UAV will promptly send an acknowledgment (ACK) to the ground station. Upon receiving the aacknowledgment the steady-state phase concludes, prompting the control module to deactivate its message receiver and transition into sleep mode, thus indicating the end of one cycle. The length and scheduling of each round are determined by the requirements of the application. Figure 8 elegantly presents a comprehensive overview of a singular round in the DICOT-CUAV routing protocol under consideration. The section labeled "Illustration of a single round of a UAV" within the dotted box visually details each step that occurs throughout this round. The figure is divided into two vertical boxes. On the left, we have "UAV-Aerial BS," illustrating processes at the UAV like CCA and *WuC* transmission. On the right, we find "Ground Sensor Node," showcasing processes at SNs such as reception, CSMA-CA, and joining request transmission. Furthermore, there are two horizontal boxes present. The upper box labeled "SETUP PHASE" involves activities such as cluster formation and TDMA slot allocation to sensor nodes. On the other hand, the lower box known as "STEADY STATE PHASE" covers tasks related to data transmission to the UAV and reception of acknowledgment (AcK) from it. The illustration clearly shows a full cycle in which all essential procedures occur in distinct boxes for

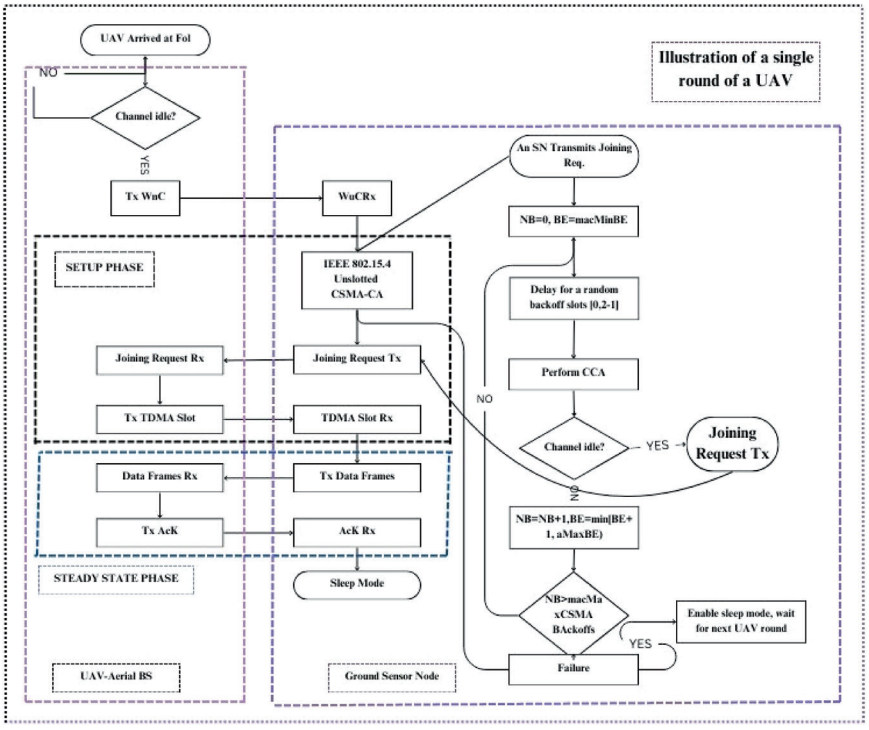

Figure 8. Diagram depicting the proposed protocol

both UAV and ground SNs. The setup phase and steady-state phase are delicately enveloped within separate dotted boxes, each one symbolizing unique stages nestled within a single round of the envisioned protocol.

The Data Flow Model includes collecting information from deployed SNs via their designated TDMA slots. Subsequently, these sensor nodes forward the data packets to the assigned Cluster Head, which happens to be an Unmanned Aerial Vehicle. To guarantee the dependable transfer of data, a protocol known as selective repeat is employed, which is a type of automatic repeat request (ARQ) protocol. In DICOT-CUAV, the SN will discard any data packets that have been acknowledged by the UAV because of memory limitations. To ensure reliability, the SN needs to resend the data packets that have been sent but not yet acknowledged in the upcoming round. Having a reliable transmission of data between Sensor Nodes and Unmanned Aerial Vehicles is essential in Wireless Sensor Networks. Factors like the duration of TDMA slots allocated by the UAV and channel behavior can affect this transmission. Ensuring consistent channel conditions is crucial for precise data transmission. Frequent shifts in channel conditions may reduce the likelihood of receiving acknowledgments (ACK) for data packets from the UAV, leading to extended waiting periods for the SN and heightened energy usage. In these circumstances, the sensor node will hold onto the data packets for the upcoming UAV encounter, unable to store any more sensed data because of its limited memory capacity. Ensuring reliable data transmission requires careful consideration of the critical aspect of the TDMA slot length set by the UAV. If the TDMA slots are too brief, it may not be possible to effectively transmit all data packets within that allocated time interval. As a result, any remaining data packets will need to be queued for the upcoming UAV cycle. Hence, it is crucial to set the TDMA slot duration in a manner that ensures the successful transmission of all data packets within the designated time frame. If the TDMA slots are excessively long, this will lead to an extended period of hovering for the UAV. To guarantee dependable data transmission, it is crucial to finely tune parameters like TDMA slot duration, channel conditions, and UAV hover time. By optimizing these parameters, we can improve the dependability of data transmission and facilitate the smooth transfer of sensed data from the Sensor Network to the Unmanned Aerial Vehicle with minimal interruptions or data losses. Figure 9 beautifully depicts the complete operational process of the DICOT-CUAV protocol.

4. PERFORMANCE ANALYSIS

4.1 NETWORK THROUGHPUT

The rate of data transfer from a sender to a receptor over, or across different locations, is often called network throughput and is measured in bits per second. It includes network latency, packet loss, and protocol factors to accurately provide real transfer speeds. High network performance means efficient use of network capacity. The proposed DICOT-CUAV model incorporates clustering and TDMA slot allocation, while the inclusion of additional data transmission slots has resulted in lower collision rates and greater total data volume. The use of CSMA-CA ensures that the probability of packet collisions is reduced. Both UAVs and SNs contribute to the prolonged lifespan of nodes through their energy consumption. This is advantageous. CCA ensures that data packets are transmitted through cleaner channels, which can increase throughput.

4.2 POWER UTILIZATION

Energy consumption refers to the amount of electrical energy utilized by a system, device, or component to operate smoothly. System efficiency and power consumption are usually measured in watts. Optimizing energy use is important to improve energy efficiency and extend the life of battery devices. The way the DICOT-CUAV model works is by regulating the energy usage of both UAVs and SNs. To conserve energy, the UAV only moves at a fixed altitude and avoids unnecessary maneuvering. Avoiding unnecessary transfer of power to SNs that already have enough energy. Only the required retransmissions are utilized by the selective replay protocol, which prevents energy wastage in duplicate data transmissions.

4.3 ENERGY EFFICIENCY

The energy efficiency of a system or device represents how effectively it can carry out its intended function while using a minimal amount of energy. This useful yield is usually

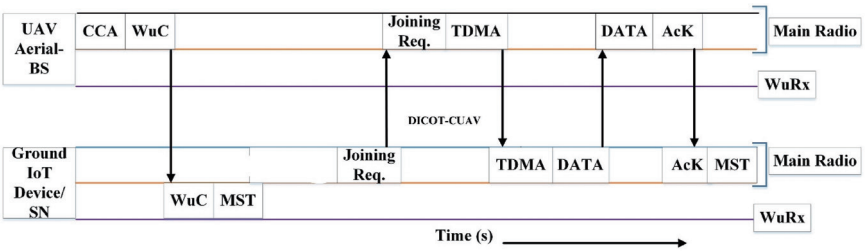

Figure 9. A visualization of the data movement in the context of DICOT-CUAV

measured as a fraction of the total energy. Improving energy efficiency reduces energy waste and operating costs. By acting as a CH, the UAVs in the DICOT-CUAV model are highly energy efficient, which reduces the long-range energy consumption needed for data transfer. By utilizing multiple TDMA slots for transmission and collecting information from local satellites, the model can reduce collisions and energy consumption, ultimately saving significant amounts of energy. Energy consumption is minimal and data is transmitted with reliability.

4.4 DATA DELIVERY RATIO

The data transmission ratio gauges the amount of information sent from a source to its intended destination. Its importance lies in the ability to measure the reliability and efficiency of data transmission through network communications. A higher data transfer ratio means more efficient and reliable data transfer. A high data transfer ratio is a key feature of the DICOT-CUAV model. Its model relies on several techniques, including cluster-based data collection, TDMA slot allocation, ARQ protocol implementation (CCA), and adaptive data aggregation to ensure consistent transmission with minimal loss. This is achieved using various approaches. High data rates in WSNs can be maintained with the proposed model.

4.5 AVERAGE DELAY

The average delay represents the duration for data packets to travel across a network from one point to another, as explained earlier. All possible delays due to processing, queuing, delivery, and forwarding are listed. A lower average delay means a more responsive and efficient network. The average delay in the DICOT-CUAV model is relatively minor. Adaptive manipulation of data aggregation and channel conditions, the model's well-structured data transmission protocols, efficient use of TDMA slots (throughput control modules), and structured communication methods make it possible to reduce the time required for transmitting data from SNs to base station UAVs. High-speed data transmission in WSNs is a desirable outcome of the proposed model.

4.6 DATA LOSS RATIO

Data loss is the proportion of packets sent to the network minus the data packet that does not make it. It measures the reliability and efficiency of data transmission. A better data loss ratio leads to more flexible and reliable networks. The DICOT-CUAV model has a low data loss ratio. Effective communication protocols, dependable delivery mechanisms, and adaptive processing of data loss conditions are all key factors in reducing the probability that data will not be lost. Reliable data transmission in WSNs is facilitated by the proposed model.

4.7 ROUTING OVERHEAD

Routing overhead is the total expenditure of network resources for maintaining and managing routing tables and routes, which is known as the cost of routing. This includes bandwidth, processing power, and time spent on tasks such as route finding and maintenance. The network's overall efficiency and effectiveness may be negatively impacted by high routing costs. Despite the DICOT-CUAV model's focus on efficient and reliable data transmission, the moderate to high routing overhead is inevitable due to dynamic clustering, UAV motion control, and channel estimation complexity. The model's objective is to achieve greater data reliability, energy efficiency, and network throughput without incurring additional overhead.

4.8 EVALUATION OF AVERAGE REWARD AND SENSING ACCURACY

Each model's performance is measured by the average reward assessment over time, which reflects the total benefit obtained. Sense accuracy evaluates each model's ability to detect or sense targets with sufficient accuracy. By using both metrics, the model's efficiency and dependability can be gauged as it moves through different time stages. Better model performance is equated to higher values.

5. RESULT AND DISCUSSION

As we discussed in the above section, we have calculated a list of performance metrics they are network throughput, power utilization, energy efficiency, data delivery ratio, average delay, data loss ratio, routing overhead, and average reward and sensing accuracy. This helps to showcase the development of DICOT-CUAV proposed with three existing techniques MOOUAV, EHUAVCR, and MUAVFD.

Figure 10, shows the throughput which compared the DICOT-CUAV proposed model with the MOOUAV model is 201.45 Kbps, the EHUAVCR model is 256.28 Kbps, the MUAVFD model with 326.17 Kbps, where our DICOT-CUAV model achieve a high value 531.89 Kbps. Which compares to high utilization of throughput. Figure 11, performs power utilization with the existing model of MOOUAV model has 256.17 Joules, the EHUAVCR model has 201.71 Joules, the MUAVFD model is 125.31 Joules, and our DICOT-CUAV model achieves low power utilization of 109.47 Joules. In Figure 12, the proposed model DICOT-CUAV model achieves a high energy efficiency of 89.74 %, when compared to our existing model MOOUAV model at 61.47 %, the EHUAVCR model achieves 69.25 %, and the MUAVFD model is 75.16 %. In Figure 13, data delivery is consumed by 96.28 % of the DICOT-CUAV proposed model. Where the existing techniques are archives 75.28 %, 81.46%, and 86.74 %. Which is compared to a high proposed

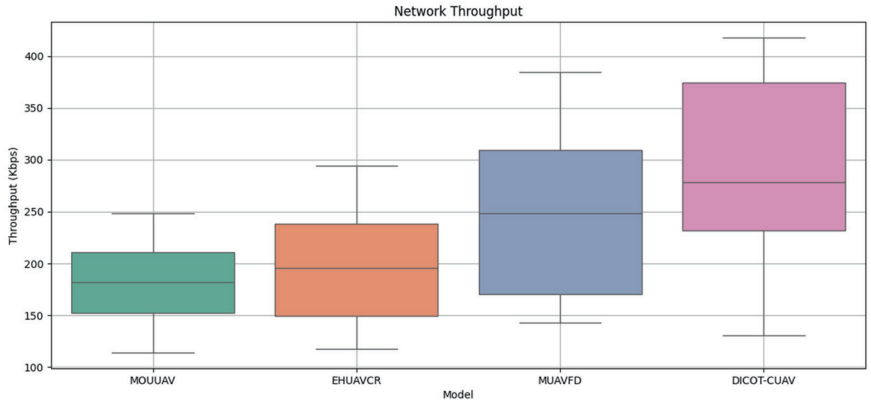

Figure 10. Network throughput

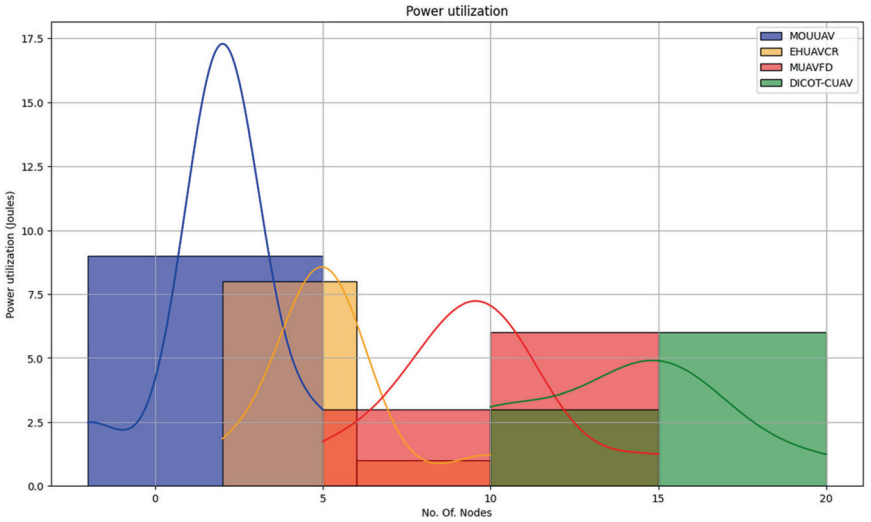

Figure 11. Power utilization

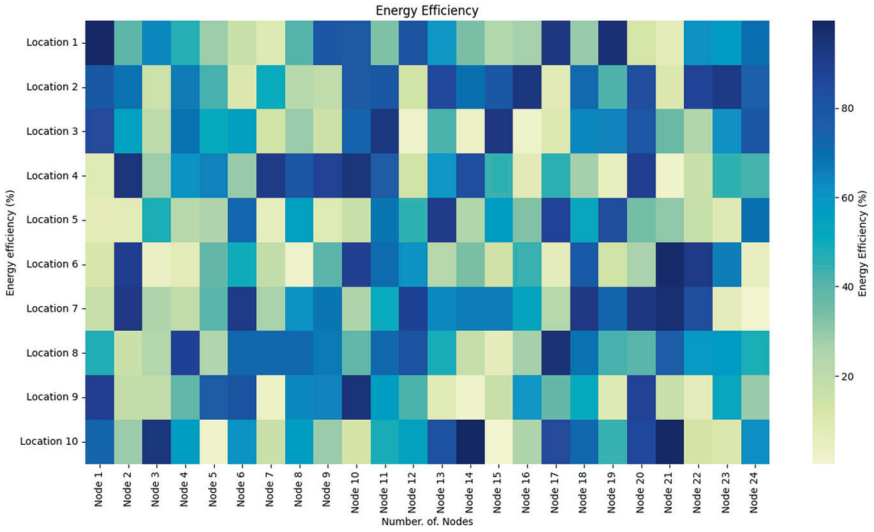

Figure 12. Energy efficiency

Figure 13. Data delivery ratio

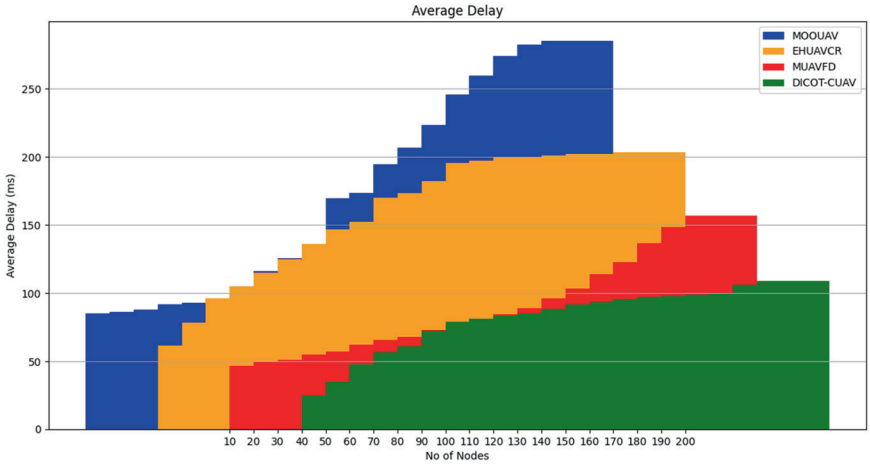

Figure 14. Average delay

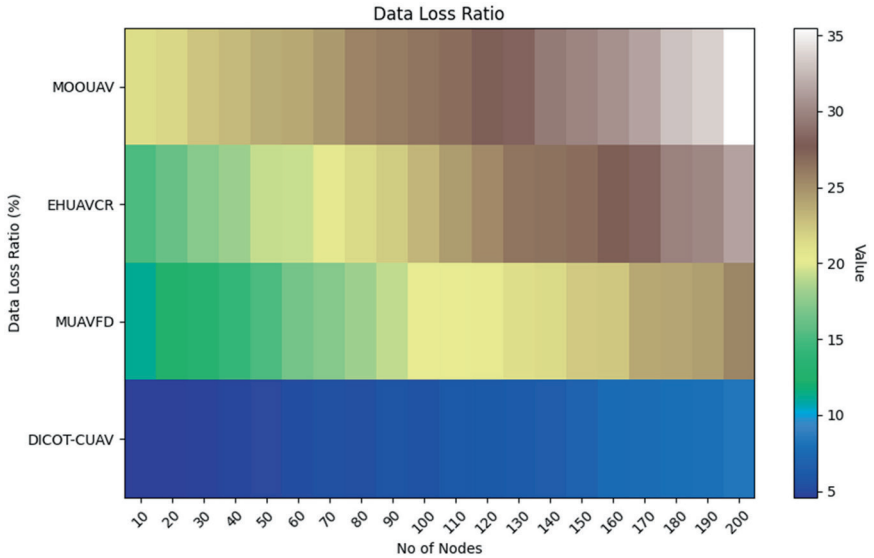

Figure 15. Data loss ratio

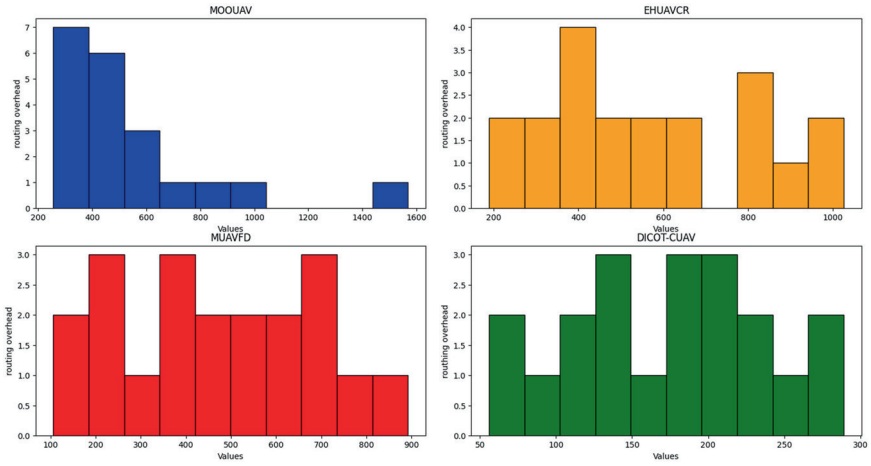

Figure 16. Routing overhead

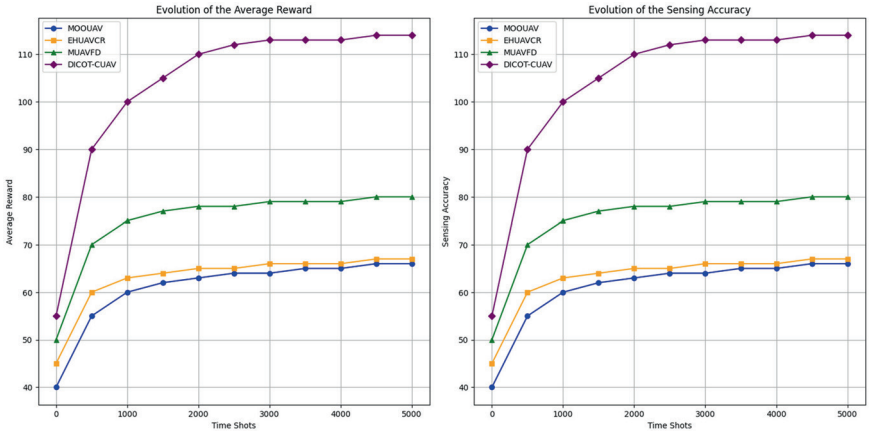

Figure 17. Average reward and sensing accuracy

model. The average delay is showcased in Figure 14, the existing techniques are archived higher than our DICOT-CUAV proposed model. Where the MOOUAV model is 285.47 ms which very higher than all other models. The EHUAVCR and MUAVFD models are 203.78 ms and 156.89 ms. Our DICOT-CUAV model is archived 109.25 ms which is less than other models. Figure 15, delivers the ratio of loss of the existing models MOOUAV model is 35.48 %, the EHUAVCR model is 31.47 %, and the MUAVFD model is 25.56 % where the DICOT-CUAV model achieves a less delay of 8.36 %. Figure 16 discusses the overhead of the MOOUAV model is archives high 1568 packets, whereas the EHUAVCR model has 1025 packets, the MUAVFD model has 892 packets, and our proposed model achieves less overhead when compared to the exiting technique's 289 packets.

The effectiveness of the DICOT-CUAV model in various network and energy efficiency metrics is demonstrated through an evaluation. The model achieves high Figure 10., throughput by utilizing efficient clustering, TDMA slot allocation, and CSMA-CA, which minimize collisions and maximize channel usage. Achieving optimal Fig 11, power utilization is possible by controlling the movement of UAVs and implementing specific retransmissions. UAVs and SN batteries can be extended using this method. UAVs that function as cluster heads save Fig 12, energy by reducing the need for extended data transfers, with additional features like TDMA slots and local data collection to minimize collisions. By utilizing cluster-based data collection, adaptive dataset aggregate, and reliable protocols, the model can deliver high levels of information with minimal loss as discussed in Fig 15. Using adaptive aggregation and efficient TDMA allocation, the Fig 14, average delay is reduced to reduce packet delivery times. By utilizing reliable communication protocols, the data loss ratio is kept within acceptable limits, which enhances the reliability of the information. Dynamic clustering and channel estimation generate a moderate to high amount of Fig 16, routing overhead, but this is offset by improved data reliability and efficiency. The prototype displays a consistently high reward level and

precise sensing performance over time, indicating its effectiveness in providing significant rewards while maintaining accuracy. By optimizing data throughput, energy consumption, and reliable data delivery effectively, DICOT-CUAV is well-suited for resource-intensive environments like WSNs.

6. CONCLUSION

An integrated system of EH-UAV-CRN that integrates both primary and secondary networks with UAVs to improve the reliability of data transmission and communication. Dynamic network conditions are effectively managed in this model using channel models and optimization algorithms. Studies on spectrum sensing and adaptive transmission strategies are centered on reducing interference while optimizing spectrum utilization, which is crucial for maintaining coexistence between primary and secondary users. To address congestion and connectivity challenges in IoT networks, the DR-UAV routing protocol is an innovative solution. This protocol provides effective disaster and environmental monitoring solutions that require reliable communication. DICOT-CUAV is a comprehensive protocol that offers optimum performance for UAV-assisted data acquisition in WSNs DICOT-CUAV's combination of dynamic clustering, TDMA scheduling, and efficient data transmission strategies allows it to tackle the challenges of energy efficiency, data reliability, network coverage, etc. A consistent cycle is created by its repeated initialization, cluster formation, and steady-state data transmission in a variety of environmental conditions, guaranteeing reliable operation. Optimal data integrity is achieved through the selective repeat ARQ mechanism, which precisely manages all retransmissions and improves system reliability. DICOT-CUAV is an essential advancement in enhancing the performance and longevity of WSN applications that are UAV-compatible. Utilizing the EH-UAV-CRN combination with the DICOT-CUAV protocol offers a complete solution for future wireless communication systems. The integration of UAV technologies with modern protocols will not only improve communications reliability and spectrum efficiency, but also provide a path for innovative uses in IoT, disaster management systems, and environmental monitoring. The well-structured blending of these technologies and protocols establishes a solid foundation for wireless network evolution, guaranteeing improved efficiency reliability as well as flexibility in harsh and ever-changing environments.

7. REFERENCES

1. MAISAM ALI, KASHIF NASEER QURESHIC, et.al,(2023). "Decision-Based Routing for Unmanned Aerial Vehicles and Internet of Things Networks", *Application Science*, *13*, 2131, doi: 10.3390/app13042131
2. BRINDHA SUBBURAJ, UMA MAHESWARI JAYACHANDRAN, et.al, (2023). "A Self-Adaptive Trajectory Optimization Algorithm Using Fuzzy Logic for Mobile Edge Computing System Assisted by Unmanned Aerial Vehicle", *Drones*, *7*, 266, doi: 10.3390/drones7040266
3. S. KASETTI AND S. KORRA, (2023) . "Multimedia Data Transmission with Secure Routing in M-IOT-based Data Transmission using Deep Learning Architecture," *Journal of Computer Allied Intelligence*, *1*(*1*), 1–13, https://doi.org/10.69996/jcai.2023001
4. HONGXIA ZHANG, SHIYU XI, et.al, (2023). "Resource Allocation and Offloading Strategy for UAV-Assisted LEO Satellite Edge Computing", *Drones*, *7*, 383, doi: 10.3390/drones7060383
5. XI WANG, SHUO SHI, et.al, (2024). "Research on Service Function Chain Embedding and Migration Algorithm for UAV IoT", *Drones*, *8*, 117, doi: 10.3390/drones8040117
6. B.ASHOK KUMAR, K.VIJAYACHANDRA, G.NAVEEN KUMAR AND V.N.LAKSHMANA KUMAR, "Blockchain Technology Communication Technology Model for the IoT," *Journal of Computer Allied Intelligence*, *2*(4), 20–35, 2024. https://doi.org/10.69996/jcai.2024017
7. JINYI ZHAO, YANBIN MEI, et.al, "Multi-Objective Optimization for EE-SE Tradeoff in Space-Air-Ground Internet of Things Networks", *Electronics*, *12*, 2585, 2023, doi: 10.3390/electronics12122585
8. SRINIVASA SAI ABHIJIT CHALLAPALLI, "Sentiment Analysis of the Twitter Dataset for the Prediction of Sentiments," *Journal of Sensors, IoT & Health Sciences*, *2*(4), 1–15, 2024. https://doi.org/10.69996/jsihs.2024017
9. SRINIVASA SAI ABHIJIT CHALLAPALLI, BALA KANDUKURI, HARI BANDIREDDI AND JAHNAVI PUDI, "Profile Face Recognition and Classification Using Multi-Task Cascaded Convolutional Networks," *Journal of Computer Allied Intelligence*, *2*(6), 65–78, 2024. https://doi.org/10.69996/jcai.2024029
10. JAEWOOK LEE, HANEUL KO, "Joint Optimization on Trajectory, Data Relay, and Wireless Power Transfer in UAV-Based Environmental Monitoring System", *Electronics*, *13*, 828, 2024, doi: 10.3390/electronics13050828b
11. SHUQI WANG, NAN QI, et.al, "Trajectory Planning for UAV-Assisted Data Collection in IoT Network: A Double Deep Q Network Approach", *Electronics*, *13*, 1592, 2024, doi: 10.3390/electronics13081592
12. XUAN-TOAN DANG, OH-SOON SHIN, "Optimization of Energy Efficiency for Federated Learning over Unmanned Aerial Vehicle Communication Networks", *Electronics*, *13*, 1827, 2024, doi: 10.3390/electronics13101827

13. MENGTANG LI, GUOKU JIA, et.al, "Efficient Trajectory Planning for Optimizing Energy Consumption and Completion Time in UAV-Assisted IoT Networks", *Mathematics*, *11*, 4399, 2023, doi: 10.3390/math11204399
14. GUOKU JIA, CHENGMING LI, et.al, "Energy-Efficient Trajectory Planning for Smart Sensing in IoT Networks Using Quadrotor UAVs", *Sensors*, *22*, 8729, 2022, doi: 10.3390/s22228729
15. SANG QUANG NGUYEN, ANH-TU LE, et.al, "Exploiting User Clustering and Fixed Power Allocation for Multi-Antenna UAV-Assisted IoT Systems", *Sensors*, *23*, 5537, 2023, doi: 10.3390/s23125537
16. SYED LUQMAN SHAH, ZIAUL HAQ ABBAS, et.al, "An Innovative Clustering Hierarchical Protocol for Data Collection from Remote Wireless Sensor Networks Based Internet of Things Applications", *Sensors*, *23*, 5728, 2023, doi: 10.3390/s23125728
17. LIHAN LIU, MENGJIAO XU, et.al, "Delay-Informed Intelligent Formation Control for UAV-Assisted IoT Application", *Sensors*, *23*, 6190, 2023, doi: 10.3390/s23136190
18. MOHAMED OULD-ELHASSEN AOUEILEYINE, RAMZI ALLANI, et.al, "Coverage Strategy for Small-Cell UAV-Based Networks in IoT Environment", *Sensors*, *23*, 8771, 2023, doi: 10.3390/s23218771
19. WEI ZHUANG, FANAN XING, et.al, "Task Offloading Strategy for Unmanned Aerial Vehicle Power Inspection Based on Deep Reinforcement Learning", *Sensors*, *24*, 2070, 2024,doi: 10.3390/s24072070
20. MOHAMED ABDEL-BASSET, REDA MOHAMED, et.al, "Evolution-based energy-efficient data collection system for UAV-supported IoT: Differential evolution with population size optimization mechanism", *Expert Systems with Applications*, *245*, 123082, 2024, doi: 10.1016/j.eswa.2023.123082
21. ZHIXIONG CHEN, JIAWEI YANG, et.al, "UAV-assisted MEC offloading strategy with peak AOI boundary optimization: A method based on DDQN", *Digital Communications and Networks*, *24*, 00015-4, 2024, doi: 10.1016/j.dcan.2024.01.003
22. PRAKHAR CONSUL, ISHAN BUDHIRAJA, et.al, "Deep Reinforcement Learning Based Reliable Data Transmission Scheme for Internet of Underwater Things in 5G and Beyond Networks", *Procedia Computer Science*, *235*, 1752–1760, 2024, doi: 10.1016/j.procs.2024.04.166
23. XUE-YONG YU, WEN-JIN NIU, et.al, "UAV-assisted cooperative offloading energy efficiency system for mobile edge computing", *Digital Communications and Networks*, *10*, 16–24, 2024, doi: 10.1016/j.dcan.2022.03.005
24. CHUAN'AN WANG, BAOZHU LI, et.al, "A UAV migration-based decision-making scheme for on-demand service in 6G network", *Alexandria Engineering Journal*, *69*, 25–33, 2023, doi: 10.1016/j.aej.2023.01.034
25. XIAOBIN XU, HUI ZHAO, et.al, "A Blockchain-Enabled Energy-Efficient Data Collection System for UAV-Assisted IoT", IEEE *Internet of Things Journal*, *8*, no. 4, pp. 2431 – 2443, 2021, doi: 10.1109/JIOT.2020.3030080
26. ALIA ASHERALIEVA, DUSIT NIYATO, "Distributed Dynamic Resource Management and Pricing in the IoT Systems With Blockchain-as-a-Service and UAV-Enabled Mobile Edge Computing", IEEE *Internet of Things Journal*, *7*, no. 3, pp. 1974 – 1993, 2023, doi: 10.1109/JIOT.2019.2961958
27. BON-HONG KOO, CHANGMIN LEE, et.al, "Molecular MIMO: From Theory to Prototype", IEEE *journal on selected areas in communications*, *34*, no. 3, pp. 600–614, 2016, doi: 10.1109/JSAC.2016.2525538
28. ZHUTIAN YANG, HANZE LIU, et.al, "UEE-RPL: A UAV-based energy-efficient routing for the internet of things", IEEE *Transactions on Green Communications and Networking*, *99*, pp. 1–1, 2021, doi: 10.1109/TGCN.2021.3085897
29. YI LIU, SHENGLI XIE, et.al, "Cooperative Offloading and Resource Management for UAV-Enabled Mobile Edge Computing in Power IoT System", IEEE *Transactions on Vehicular Technology*, *69*, pp. 10, pp. 12229 – 12239, 2020, doi: 10.1109/TVT.2020.3016840
30. ZIJIE WANG, RONGKE LIU, et.al, "Energy-Efficient Data Collection and Device Positioning in UAV-Assisted IoT", IEEE *Internet of Things Journal*, *7*, no. 2, pp. 1122 – 1139, 2020, doi: 10.1109/JIOT.2019.2952364
31. HENGSHUO LIANG, WEICHAO GAO, et.al, "Internet of Things Data Collection Using Unmanned Aerial Vehicles in Infrastructure Free Environments", IEEE *Access*, *8*, pp. 3932–3944, 2019, doi: 10.1109/ACCESS.2019.2962323
32. YONGJUN XU, ZIJIAN LIU, et.al, "Robust Resource Allocation Algorithm for Energy-Harvesting-Based D2D Communication Underlaying UAV-Assisted Networks", IEEE *Internet of Things Journal*, *8*, no. 23, pp. 17161–17171, 2021, doi: 10.1109/JIOT.2021.3078264
33. SENHAO ZHAO, HANG HU, YANGCHAO HUANG, et.al, "Optimization of Effective Throughput in NOMA-Based Cognitive UAV Short-Packet Communication", *Application Science*, *13*, pp. 599, 2023, doi: 10.3390/app13010599
34. LIANG ZHOU, WEIQIANG XU, et.al, "RIS-Enabled UAV Cognitive Radio Networks: Trajectory Design and Resource Allocation",

Information, *14*, pp. 75, 2023, doi: 10.3390/info14020075c

35. LINGTONG MIN, JIAWEI LI, et.al, "Secure Rate-Splitting Multiple Access for Maritime Cognitive Radio Network: Power Allocation and UAV's Location Optimization", *J. Mar. Sci. Eng.*, *11*, pp. 1012, 2023, doi: 10.3390/jmse11051012
36. WAQAS KHALID, HEEJUNG YU, et.al, "Residual Energy Analysis in Cognitive Radios with Energy Harvesting UAV under Reliability and Secrecy Constraints", *Sensors*, *20*, pp. 2998, 2022, doi: 10.3390/s20102998
37. AMR AMRALLAH, EHAB MAHMOUD MOHAMED, et.al, "Enhanced Dynamic Spectrum Access in UAV Wireless Networks for Post-Disaster Area Surveillance System: A Multi-Player Multi-Armed Bandit Approach", *Sensors*, *21*, pp. 7855, 2021, doi: 10.3390/s21237855
38. WEIHENG JIANG, WANXIN YU, et.al, "Multi-Agent Reinforcement Learning for Joint Cooperative Spectrum Sensing and Channel Access in Cognitive UAV Networks", *Sensors*, *22*, pp. 1651, 2022, doi: 10.3390/s22041651
39. MUHAMMAD RASHID RAMZAN, MUHAMMAD NAEEM, et.al, "Radio resource management in energy harvesting cooperative cognitive UAV assisted IoT networks: A multi-objective approach", *Digital Communications and Networks*, *23*, pp. 00019–6, 2023, doi: 10.1016/j.dcan.2023.01.006
40. HE XIAO, HONG JIANG, et.al, "Energy efficient resource allocation in delay-aware UAV-based cognitive radio networks with energy harvesting", *Sustainable Energy Technologies and Assessments*, *45*, pp. 101204, 2021, doi: 10.1016/j.seta.2021.101204
41. ABDENACER NAOURI, HUANSHENG NING, et.al, "Maximizing UAV fog deployment efficiency for critical rescue operations: A multi-objective optimization approach", *Future Generation Computer Systems*, *159*, pp. 255–271, 2024, doi: 10.1016/j.future.2024.05.007